

Pr and Cr co-doped BiFeO₃ nanotubes: an advance multiferroic oxide material

Rajasree Das, Gobinda Gopal Khan and Kalyan Mandal

Department of Material Sciences, S. N. Bose National Centre for Basic Sciences, Block-JD, Sector-III, Salt Lake City, Kolkata -700 098, India

Abstract. Arrays of single phase pure and Pr-Cr co-doped BiFeO₃ (BFO) nanotubes (NTs) with compositions BiFeO₃ and Bi_{0.9}Pr_{0.1}Fe_{0.9}Cr_{0.1}O₃ have been synthesized using Anodic Aluminium Oxide (AAO) template (pore diameter ~250 nm) by wet chemical liquid phase deposition technique. All the NTs show ferromagnetic nature at room temperature (RT). Better magnetic properties are observed in the co-doped BFO NTs with the value of saturation magnetization (M_S) ~ 49 memu/g, magnetization at the remanence (M_R) ~12 memu/g and coercive field (H_C) ~103 Oe. Increase of ferromagnetic signature in the co-doped BFO NTs is believed to be due to the collapse of the space-modulated spin structure. Significant increase in the dielectric characteristics in co-doped BFO NTs suggests lowering of leakage current due to the reduction of the oxygen vacancies in the structure. Strong Magnetodielectric effect (MD), expressed by $[\epsilon_r(H) - \epsilon_r(0)]/\epsilon_r(0)$ is observed in doped BFO NTs, where the increase of the dielectric constant is noticeable with the increase in the applied magnetic field. The co-doped BFO NTs show noticeable increase in MD effect at a lower field (1-2 kOe).

1 Introduction

Among all the multiferroic materials, Bismuth ferrite (BFO) has drawn intense research attention because of the coupling between their magnetic and electric properties which is known as magnetoelectric (ME) effect: An applied external magnetic field causes the electric dipoles to reorient, giving rise to a net change in the polarization of the materials. Hence, BFO is a promising candidate for their potential application in electronic devices like multiple-state memories, magnetic data-storage media, actuators, transducers, sensors and spintronic devices [1-5]. But it has been a challenge to get good magnetoelectric coupling at room temperature (RT) in bulk BFO compounds which is necessary for the practical applications. In this regard, it has been reported by several groups that the single crystalline and nanostructure BFO exhibits enhanced size dependent magnetic and ferroelectric properties [6,7,8-12]. Enhancement in the resistance provides better ferroelectric properties to the transition metal ions such as Cr³⁺ and Mn³⁺ doped BFO thin films [7,13,14]. It has been also reported that Pr and La doping improve ferromagnetic and ferroelectric properties of BFO thin films due to the structural modification and reduction of the oxygen vacancies, respectively [15-18].

Continuing this search to get a better multiferroic material, in this present work we have reported the structural, magnetic, dielectric and magnetodielectric properties of Pr-Cr co-doped BFO nanotubes (NTs) synthesized on AAO template via an easy wet chemical liquid phase deposition (LPD) technique.

2 Experimental details

The arrays of BFO and co-doped BFO NTs are grown on self-ordered nanoporous anodic aluminium oxide (AAO) template, fabricated by two stage electrochemical anodization of high purity (99.99%) aluminium foil by critically controlling the anodization parameters, as reported elsewhere [19]. High purity equimolar bismuth nitrate [Bi(NO₃)₃ · 5H₂O] and ferric nitrate [Fe(NO₃)₃ · 9H₂O] are dissolved into 2-methoxyethanol (C₃H₈O₂) followed by constant stirring of the mixture for about 30 min at RT to make a clear solution of BFO. The concentration and pH of the final solution have been adjusted to 0.3 M and 1–2, respectively. The AAO templates with pore diameter ~ 250 nm are immersed inside the solution for 3 days to help the solution to reach inside the pores of the template. After removing the templates from the solution the surface has been washed with water carefully to remove the BFO solution from the template surface and it has been dried under IR lamp. To crystallize the samples into perovskite structure, the AAO templates filled with BFO solution have been annealed at 500°C for 2 hr in air. For synthesizing the Pr and Cr co-doped BFO NTs, the procedure is similar with the undoped BFO. Here an appropriate stoichiometric amount of praseodymium nitrate (Pr(NO₃)₃ · 6H₂O) and chromium nitrate [Cr(NO₃)₃ · 9H₂O] solution are added to the solution of bismuth nitrate and ferric nitrate to fabricate the Cr-Pr co-doped BFO NTs (Bi_{0.9}Pr_{0.1}Fe_{0.9}Cr_{0.1}O₃ (Pr_{0.1}Cr_{0.1}BFO)).

3 Results and discussion

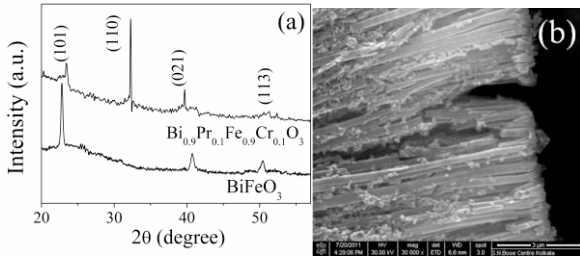


Fig. 1. (a) XRD pattern of the undoped and co-doped BFO NTs and (b) SEM image of the $\text{Pr}_{0.1}\text{Cr}_{0.1}\text{BFO}$ NTs.

3.1. Structural properties

The crystallographic phases of all the undoped and co-doped BFO NTs are shown in Fig. 1(a). All the peaks correspond to rhombohedral structure with R-3m space group of the pure and doped BFO NTs with no considerable impurity peaks. Co-doped NTs show strong (110) peak around $2\theta \sim 32^\circ$. Whereas, this peak is absent in the XRD pattern of pure BFO NTs. After doping the BFO NTs prefer to grow along [110] direction than its [101] direction.

Figure 1(b) shows the representative low magnification FESEM image of the bunch of as prepared $\text{Pr}_{0.1}\text{Cr}_{0.1}\text{BFO}$ NTs released from AAO template by dissolving the template in 2 M NaOH solution. It can be seen from the figure that the outer surface walls of the NTs are very smooth. All the NTs are found to have very similar average length ($\sim 4\text{--}5\ \mu\text{m}$) and uniform outer diameter ($\sim 250\ \text{nm}$) and tube wall thickness of about 50 nm with the aspect ratios in the range of 16–20.

3.2 Magnetic properties

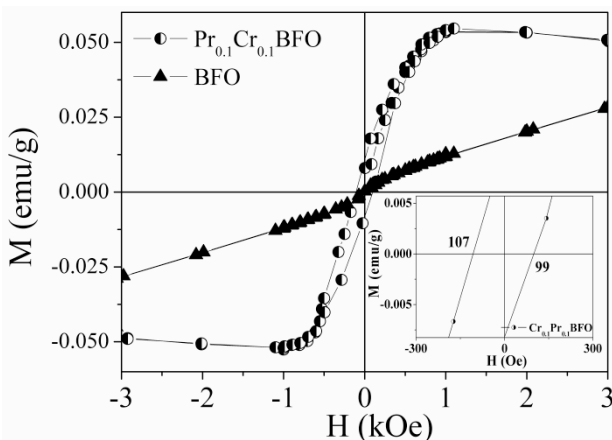


Fig. 2. Field dependence of magnetization for the pure and co-doped BFO NTs upto $\pm 3\ \text{kOe}$ at 300 K.

Figure 2 shows the Magnetization (M) versus applied magnetic field (H) plot for undoped and co-doped BFO NTs at RT after subtracting the diamagnetic contribution of AAO template. It is evident that the pure BFO NTs show weak ferromagnetism (FM) at RT, whereas, the

$\text{Pr}_{0.1}\text{Cr}_{0.1}\text{BFO}$ NTs exhibit enhanced FM ordering with saturation near 1 kOe. The saturation magnetization (M_S), magnetization at the remanence (M_R) and coercive field (H_C) values of the $\text{Pr}_{0.1}\text{Cr}_{0.1}\text{BFO}$ NTs are 49 memu/g, 12 memu/g and 103 Oe, respectively.

It is well known that bulk BFO shows antiferromagnetic response because G type antiferromagnetic [20] spin ordering in addition to the spiral spin structure with wavelength of 62 nm, cancels the macroscopic magnetization in bulk BFO. While BFO NTs shows weak ferromagnetism due to size effect as reported in case of other nanostructures [6,7] too. Here, the huge enhancement in the magnetization of $\text{Pr}_{0.1}\text{Cr}_{0.1}\text{BFO}$ NTs is believed to be due to the change in canting angle [21] or suppression of the complicated spiral spin structure [16] along with coupling interaction between the Fe^{3+} and Cr^{3+} ions [22] in the compound.

3.3 Dielectric properties

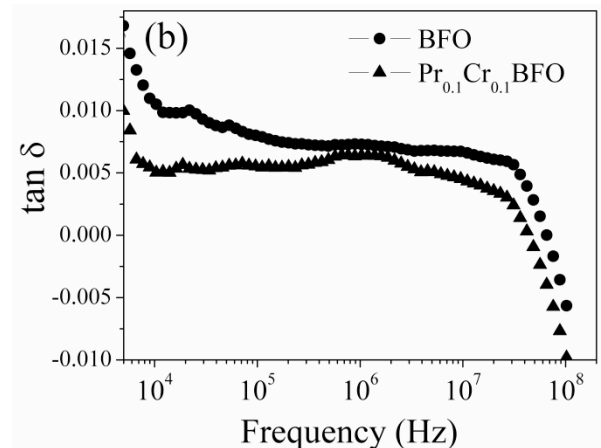
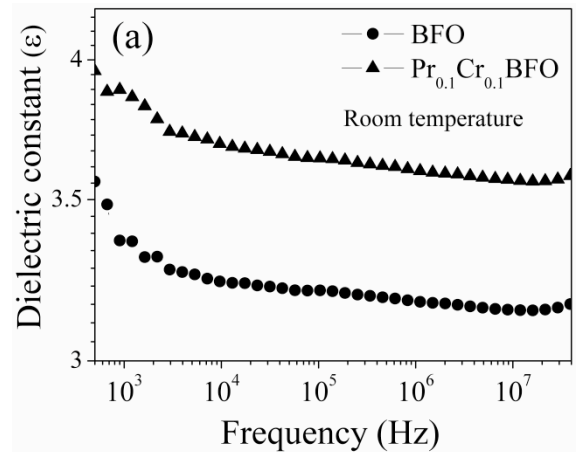


Fig. 3 (a) Dielectric constant (ϵ) and 3(b) Dielectric loss ($\tan \delta$), for the pure and co-doped BFO NTs.

RT dielectric constant (ϵ) of the undoped and co-doped BFO NTs as a function of frequency in the range from 40 Hz to 10 MHz is shown in Fig. 3(a). Very small external electric field ($E_0=500\ \text{mV}$) is applied during dielectric constant measurements. It shows strong frequency

dependence in the low frequency range, while relaxation of the dipoles is observed in the 100 kHz to 90 MHz frequency range. It is found that the $\text{Pr}_{0.1}\text{Cr}_{0.1}\text{BFO}$ NTs exhibit higher value of dielectric constant compared to the undoped BFO NTs.

Fig. 3(b) shows the variation of dielectric loss ($\tan \delta$) with frequency of the samples. It can be noticed clearly that $\tan \delta$ value is high in case of undoped BFO NTs. No relaxation peak is observed in the samples. This may be evident that the Maxwell–Wagner space charge effect does not dominate the dielectric behaviour of the NTs. For all the NTs, $\tan \delta$ value reduces with increase in the frequency with a sharp decrease around 30 MHz.

This result indicates that the oxygen vacancies in the co-doped BFO NTs is reduced considerably as the electrical properties in BFO are related to the pinning effects of space charge originated due to the presence of the oxygen vacancies [23]. Volatility of Bi plays a big role in appearance of oxygen vacancy in BFO samples during the high temperature annealing of the samples. Hence, doping Pr^{3+} replacing Bi^{3+} reduces oxygen vacancies in the BFO structure [16]. Also Cr^{3+} doping in place of Fe ion reduces the probability of existence of Fe^{2+} in the compound. So we expect that leakage current in the co-doped sample is reduced as oxygen vacancy and mix valance of Fe gives rise to leakage current in the compound.

3.4 Magnetoelectric coupling

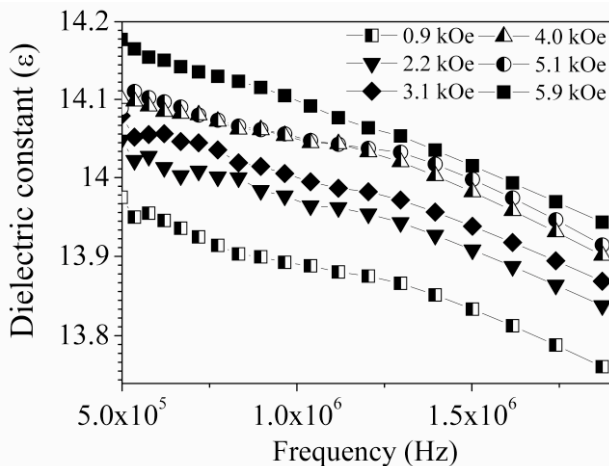


Fig. 4. Frequency dependence dielectric constant (ϵ) of the $\text{Pr}_{0.1}\text{Cr}_{0.1}\text{BFO}$ NTs at different applied magnetic field.

As discussed earlier, in multiferroics magnetic and electric domains are coupled with each others, electric order parameter of the material can be manipulated by the application of magnetic field and vice versa. In our work, we have observed the change in dielectric constant (ϵ) with the change in applied magnetic field which is a popular way to check the magnetoelectric coupling in the multiferroics. Application of external magnetic field in a magnetic material can induce strain which induces stress inside the material and generates an electric field on the ferroelectric domain. Therefore, the electrical property of

the material is modified by magnetic field. Figure 4 shows the change in ϵ value as a function of frequency of the $\text{Pr}_{0.1}\text{Cr}_{0.1}\text{BFO}$ NTs with the increase in applied magnetic field.

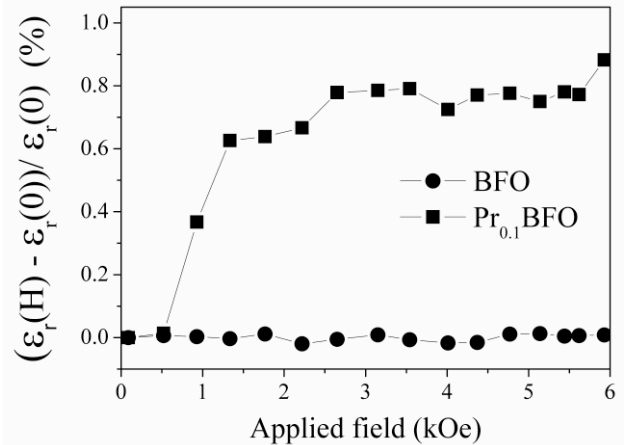


Fig. 5. Change in Magnetodielectric effect with applied field of the pure and $\text{Pr}_{0.1}\text{Cr}_{0.1}\text{BFO}$ NTs measured at frequency (f) of 1 kHz at RT.

RT magnetic field dependence of the magnetodielectric (MD) effect, expressed by $[\epsilon_r(H) - \epsilon_r(0)]/\epsilon_r(0)$ at the frequency (f) of 1 kHz for the pure and co-doped BFO NTs array are shown in Fig.5. It is clear from the plot that the pure BFO NTs does not show any variation in the MD effect up to the maximum applied field 6 kOe but $\text{Pr}_{0.1}\text{Cr}_{0.1}\text{BFO}$ NTs exhibit noticeable enhancement in the MD effect with the applied magnetic field. This MD value is comparable with the MD value of Ba doped BFO thin film and other multiferroic materials reported earlier [24–26].

4 Conclusions

In this report, pure and Pr-Cr co-doped BFO NTs with high aspect ratio are successfully fabricated within the pores of the AAO template by a facile wet chemical liquid phase deposition template assisted route. All the samples have uniform outer diameter of ~ 250 nm and wall thickness of ~ 50 nm. All the NTs crystallize to a perovskite type structure with the space group R-3m. Magnetic hysteresis loops show that Pr-Cr co-doping can substantially increase the magnetization value of BFO NTs due to the change in the canting angle and the suppression of spiral spin structure as a result of distortion created by doping large size Pr ion and the strong coupling interaction between the Fe^{3+} and Cr^{3+} ions. Noticeable improvement in the dielectric property is observed in the $\text{Pr}_{0.1}\text{Cr}_{0.1}\text{BFO}$ NTs where the enhancement may be attributed to the reduction of the concentration of oxygen vacancies due to doping. Dielectric constant of the co-doped sample increases with the increase in the applied magnetic field. Significant enhancement in the magnetodielectric behavior of the

$\text{Pr}_{0.1}\text{Cr}_{0.1}\text{BFO}$ NTs, which signifies the magnetoelectric coupling, establishes the co-doped BFO NTs as a potential multiferroic material.

Acknowledgement

One of the authors (RD) thanks Council of Scientific and Industrial Research (CSIR), Government of India, for providing financial support through a research fellowship. The authors also thank Dr. D. Das and Mr. PV Rajesh, IUC, Kolkata, India, for providing us with the SQUID measurement facility.

References

1. J. Wang *et al.*, Science 299, 1719 (2003)
2. M. Fiebig, T. Lottermoser, D. Fröhlich, A. V.Goltsev, and R. V. Pisarev, Nature 419, 815 (2002)
3. W. Eerenstein, N. D. Mathur, and J. F. Scott, Nature 442, 759 (2006)
4. N. Hur, S. Park, P. A. Sharma, J. S. Ahn, S. Guha, and S.-W. Cheong, Nature 429, 392 (2004)
5. S. X. Dong, J. Y. Zhai, J. F. Li, D. Viehland, and M. I. Bichurin, Appl. Phys. Lett., 89, 243512 (2006)
6. T.-J. Park, G. C. Papaefthymiou, A. J. Viescas, A. R. Moodenbaugh, and S. S.Wong, Nano Lett. 7, 766 (2007)
7. D. P. Dutta, O. D. Jayakumar, A. K. Tyagi, K. G. Girija, C. G. S. Pillai, and G. Sharma, Nanoscale 2, 1149 (2010)
8. X. Y. Zhang, C. W. Lai, X. Zhao, D. Y. Wang, and J. Y. Dai, Appl. Phys. Lett. 87, 143102 (2005)
9. F. Gao, Y. Yuan, K. F. Wang, X. Y. Chen, F. Chen, J.-M. Liu, and Z. F. Ren, Appl. Phys. Lett. 89, 102506 (2006)
10. Y. Du, Z. X. Cheng, S. X. Dou, D. J. Attard, and X. L. Wang, J. Appl. Phys. 109, 073903 (2011)
11. R. Mazumder, P. S. Devi, D. Bhattacharya, P. Choudhury, A. Sen, and M. Raja, Appl. Phys. Lett. 91, 062510 (2007)
12. Y.-Q. Kang, M.-S. Cao, J. Yuan, and X.-L. Shi, Mater. Lett. 63, 1344 (2009)
13. H. Naganuma, J. Miura, and S. Okamura, Appl. Phys. Lett. 93, 052901 (2008)
14. Y. Du, Z. X. Cheng, S. X. Dou, M. Shahbazi, and X. L. Wang, Thin Solid Films 518, e5 (2010)
15. B. Yu, M. Li, Z. Hu, L. Pei, D. Guo, X. Zhao, and S. Dong, Appl. Phys. Lett. 93, 182909 (2008)
16. P. Uniyal, and K. L. Yadav, J. Phys.: Condens. Matter. 21, 405901 (2009)
17. C. Lan, Y. Jiang, and S. Yang, J. Mater. Sci. 46, 734 (2011)
18. Y. H. Lee, J. M. Wu, and C. H. Lai, Appl. Phys. Lett. 88, 042903 (2006)
19. G. G. Khan, N. Mukherjee, A. Mondal, N.R. Bandyopadhyay, and A. Basumallick, Mater.Chem. Phys. 122, 60 (2010).
20. P. Fischer, M. Polomska, I. Sosnowska, and M. Szymanski, J. Phys. C 13, 1931 (1980)
21. J. Wang *et al.*, Science 307, 1203 (2005)
22. B. -C. Luo, C. -L. Chen, and K. -X. Jin, Solid State Communications 151, 712 (2011)
23. Y. Noguchi, and M. Miyayama, Appl. Phys. Lett. 78, 1903 (2001).
24. D. H. Wang, W. C. Goh, M. Ning, and C. K. Ong, Appl. Phys. Lett. 88, 212907 (2006).
25. M. Li, M. Ning, Y. Ma, Q. Wu, and C. K. Ong, J. Phys. D: Appl. Phys. 40, 1603 (2007)
26. T. Kimura, S. Kawamoto, I. Yamada, M. Azuma, M. Takano, and Y. Tokura, Phys. Rev. B 67, 180401 (2003)